J Ther Eng, Vol. 11, No. 4, pp. 1148−1159, July, 2025

Journal of Thermal Engineering
Web page info: https://jten.yildiz.edu.tr
DOI: 10.14744/thermal.0000969

Research Article

Numerical investigation of slip flow and temperature jump of nanofluid in a microchannel with square obstacles using lattice Boltzmann method

Habib KARIMI[1,*], Kourosh JAVAHERDEH[2]

[1]*Department of mechanical engineering, Roudsar and Amlash branch, Islamic Azad University, Roudsar, 44, Iran*
[2]*Faculty of mechanical engineering, university of Guilan, Rasht, 43, Iran*

ARTICLE INFO

Article history
Received: 30 April 2024
Revised: 24 September 2024
Accepted: 25 September 2024

Keywords:
Heat Transfer; Lattice Boltzmann Method; Microchannel; Nanofluid; Square Obstacles

ABSTRACT

This study investigated a forced convection of nanofluid in a microchannel with the presence of square obstacles using lattice Boltzmann method. The slip boundary conditions for velocity and temperature jump are considered for microchannel. The study is conducted in three volume fractions of nanoparticles, two Knudsen numbers and two Reynolds numbers. The results is shown that with enhancing the volume fraction of nanoparticles, the heat transfer coefficient increases more than two times. It is observed that by increasing the Knudsen number, the velocity slip and also temperature jump increases, but the heat transfer coefficient and the friction coefficient decreases. The first obstacle in the microchannel is more effective which is due to the creation of the vortex and the vortex characteristics in dissembling the hydraulic and thermal boundary layers. Also, increasing the nanoparticles volume fraction, the heat transfer coefficient rises noticeably.

Cite this article as: Karimi H, Javajerdeh K. Numerical investigation of slip flow and temperature jump of nanofluid in a microchannel with square obstacles using lattice Boltzmann method. J Ther Eng 2025;11(4):1148−1159.

INTRODUCTION

With the growth of science and the advancement of technology in the recent years, micro and nano systems are increased rapidly. These systems have great and different applications such as micro sensors and micro valves and micro pumps. Investigation of the flow and the heat transfer in microsystems has been considered by many researchers. When the dimensions of a system reach to micro scale, the ratio of surface to volume increases dramatically [1]. Therefore the surface phenomena overcome other phenomena. Simulation of microscopic phenomena flow is different from the macroscopic flow. As a suitable example it can be refer to the effect of velocity slip and temperature jump. Also, when the dimensions of a geometry is small, the molecules dimensions and the distance between them become important and there is a need to introduce a new index named the Knudsen number. Knudsen number is the ratio of mean free path of molecules to the characteristic length. Whenever Kn<0.001, the fluid flow will be continuum and the Navier Stocks equation can be used using velocity no slip boundary condition. But as 0.001<Kn<0.1, 0.1<Kn<10, and Kn>10, the fluid flow is respectively similar to the slip

***Corresponding author.**
*E-mail address: habib_karimi63@yahoo.com

This paper was recommended for publication in revised form by Editor-in-Chief Ahmet Selim Dalkılıç

flow, transition flow and free molecule flow [2-4]. This flow regimes often take place in electro mechanic systems (MEMS) and they must be examined by methods based on particles such as molecular dynamic (MD) and direct simulation of Mont Carlo (DSMC). The high computational expenses and complicated mathematical equations of MD and DSMC methods has made researchers to look for a suitable and strong alternative approach as lattice Boltzmann method (LBM) for simulation of macro and micro flows [5-7]. In addition to methods based on particle movements (particle based methods) for simulation of flow and heat transfer of a slip flow, the classic equation of Navier stocks is also used as a basic equation. But it should be mentioned that the velocity slip and temperature jump boundary conditions should be used in this case [8]. Chamkha et al. [9] studied a mixed convection of nanofluid in a cone with porous medium. They showed effect of nanoparticles on local Nusselt and Sherwood numbers. Also they investigated effects of Brownian motion for nano particles. Considering the high importance of heat transfer in microchannels, several investigations have been conducted about this issue [10-13]. Arabpour et al [10] studied laminar heat transfer of nanofluids on micro channel. They used range of Reynolds number between 1 and 100. They showed Nusselt umber is increased by increasing volume friction and Reynolds number. Mohammed et al. [11] investigated heat transfer in a square micro channel heat exchanger. They showed that thermal properties and pressure drop are increased using nanofluids. Lv et al. [12] done wide researches for optimization and dissipation performance on microchannel with heat sink. Qazi zade et al. [13] numerically investigated the effects of variable physical properties on the flow and heat transfer characteristics of simultaneously developing slip-flow in rectangular microchannels with constant wall temperature. They revealed the degree of discrepancy varies for different cases depending on Knudsen number, aspect ratio and the temperature difference between the channel inlet and the wall. Also, their results shown that even low temperature differences can alter the friction and heat transfer coefficients considerably. Adding a surface or an obstacle in microchannels is customary for better mixing of fluid flow. Simulation of vortex phenomena surrounding the sharp corners of obstacles in MEMS is of high importance [14] which may leads to increasing the heat transfer coefficient. Sharp et al. [15] used the induced-charge electroosmotic/pressure driven flow to control the positional flow near the obstacles in a microchannel. Also Berra [16] have simulated the induced-charge electroosmotic flow near an obstacle in a microchannel. They solved the nonlinear equations of Navier stocks, Nernst Planck and Poisson using finite volume method and velocity slip boundary condition. Considering the importance of heat transfer around the obstacles and microchannels and lack of suitable experimental results in different flow conditions, it is necessary to study about this issue and present results with suitable precision. One methods of increasing the heat transfer is using nanofluids as the operating fluid. Nanofluid is a result of adding solid nanoparticles to a liquid as water, oil or ethylene glycol. Roy et al. [17] numerically investigated the hydrodynamic and thermal fields of a water–Al_2O_3 nanofluid in a radial laminar flow cooling system. They showed that considerable heat transfer enhancement is possible, even achieving a twofold increase in the case of a 10% nanoparticle volume fraction nanofluid. Also, they revealed an increase in wall shear stress was also noticed with an increase in particle volume concentration. Ho et al. [18] investigated heat transfer in micro channel with heat source by nanofluid. They showed that heat transfer coefficient is more than some resistances. Tsai and Chein [19] studied a micro channel performance with heat sources and various nanofluids. They found that difference temperature is reduced between heated wall and nano particles. Jang et al. [20] studied nanofluid flow on micro channel with heat sink and found that heat transfer using nanofluids is increased about 10% compared with base fluid. Alipour et al. [21] simulated heat transfer nanofluid in a microchannel and studied effect of temperature jump on Nusselt numbers. Santra et al. [22] studied the effect of copper–water nanofluid as a cooling medium to simulate the heat transfer behaviour in a two-dimensional (infinite depth) horizontal rectangular duct, where top and bottom walls are two isothermal symmetric heat sources. They observed that the heat transfer augmentation is possible using nanofluid in comparison to conventional fluids for both the cases. Also, they revealed that the rate of heat transfer increases with the increase in flow as well as increase in solid volume fraction of the nanofluid. The lattice Boltzmann method is a rather new and applicable method for solving the nonlinear differential equations and simulation of nanofluids. It has been showed recently that this technique is a precise method of computational dynamic fluid (CFD) which provides solving complicated geometrics with minimal computation expenses [23]. LBM provides greater numerical stability using the internal energy distribution function and also included the heat discharge. Due to existence of both hydrodynamic and thermal conditions in one grid, the boundary conditions are simulated simply [24]. LBM has been used by several researchers in order to simulate the fluid flow in microchannels. Agarwal et al. [25] studied a simulation of heat transfer in microchannel with non-Newtonian fluids using LBM method. Their results were compared numerical solution with FLUENT software and showed there are agree well each other. Navidbakhsh et al. [26] studied a model of capsule migration in microchannel with LBM method.

In this study, the slip flow of a nanofluid is studied in a microchannel with the presence of two obstacles using lattice Boltzmann method. The velocity slip and temperature jump boundary conditions are used for the simulations. The nanofluid is made up of water and percentages of different volume fractions of aluminum dioxide (Al_2O_3) nanoparticles. In order to make difference in nanofluid

characteristics, a stable temperature distribution on the upper and lower walls is applied. In this work, the flow and heat transfer of a nanofluid in a microchannel with the presence of two obstacles is studied by lattice Boltzmann method. The velocity slip and temperature jump boundary conditions are used for numerical simulation.

BASIC EQUATIONS

Nanofluid

Nanofluid is a homogenous mixture of the liquid (water) and the solid particles (Al_2O_3). Also, it is supposed that the fluid is Newtonian and incompressible and the flow regime is laminar. The nanoparticles are spherical and the diameter of each particle is 100 nanometer (100 nm). Moreover, the glow effects are neglected. The effect of different volume fractions of nanoparticles on the forced convection of nanofluid in a microchannel with presence of obstacles is studied. The effective density of nanofluid in the reference temperature is presented as [27]:

$$\rho_{nf,0} = (1-\phi)\rho_{f,0} + \phi\rho_{s,0} \tag{1}$$

ϕ is the volume fraction of nanoparticles. The thermal capacity of nanofluid $(C_p)_{nf}$ can be written as follows:

$$(\rho C_P)_{nf,0} = (1-\phi)(\rho C_P)_{f,0} + \phi(\rho C_P)_{s,0} \tag{2}$$

Also, the effective viscosity of nanofluid is defined as:

$$\mu_{nf} = \frac{\mu_f}{(1-\phi)^{2.5}} \tag{3}$$

Table 1. Properties of fluid and the solid particles [27]

Properties	Water	Al_2O_3
C_p (J/kg.K)	4179	765
ρ (kg/m^3)	997	3970
k (W/m.K)	0.613	40
μ (kg/m.s)	89×10^{-5}	-
ε_r (C^2/J.m)	7.0832×10^{-6}	-

In addition, the properties of the fluid and the solid particles are shown in Table 1.

In addition to that, the effective thermal conductivity (k_{eff}) is determined with the model of Patel et al. [28]. For nanofluids with suspended spherical particles, this model is as follows:

$$\frac{k_{eff}}{k_f} = 1 + \frac{k_P A_P}{k_f A_f} + ck_P Pe \frac{A_P}{k_f A_f} \tag{4}$$

where:

$$\frac{k_P A_P}{k_f A_f} = \frac{d_f}{d_P}\frac{\phi}{(1-\phi)} \tag{5}$$

and also the Peclet number is defined as:

$$Pe = \frac{u_P d_P}{\alpha_f} \tag{6}$$

Where u_P is the Brownian motion velocity and is defines as below [28]:

$$u_P = \frac{2k_b T}{\pi\mu_f {d_P}^2} \tag{7}$$

Which k_b is the Boltzmann number (1.3807×10^{-3} J/K) [28]

Flow equations

The momentum equation and flow energy without considering body force and gravity is as follows [29]:

$$\nabla\cdot(\rho U) = 0 \tag{8}$$

$$\rho(U.\nabla U) = -\nabla P + \mu\nabla^2 U \tag{9}$$

$$\rho C_p(U.\nabla T) = k\nabla^2 T \tag{10}$$

To make dimensionless the momentum and energy equation, four dimensionless parameters for velocities, pressure and temperature are determined as below:

$$\bar{u} = \frac{u}{U_{ref}},\quad \bar{v} = \frac{v}{U_{ref}},\quad \bar{P} = \frac{P}{\rho U_{ref}^2},\quad \bar{T} = \frac{T}{T_m} \tag{11}$$

where T_m is the average temperature.

The dimensionless form of the momentum and energy equations in the x and y directions are shown in equations (12), (13) and (14):

$$\left(\bar{u}\frac{\partial\bar{u}}{\partial\bar{x}} + \bar{v}\frac{\partial\bar{u}}{\partial\bar{y}}\right) = -\frac{\partial\bar{P}}{\partial\bar{x}} + \frac{1}{\mathrm{Re}}\left(\frac{\partial}{\partial\bar{x}}\left(\frac{\partial\bar{u}}{\partial\bar{x}}\right) + \frac{\partial}{\partial\bar{y}}\left(\frac{\partial\bar{u}}{\partial\bar{y}}\right)\right) \tag{12}$$

$$\left(\bar{u}\frac{\partial\bar{v}}{\partial\bar{x}} + \bar{v}\frac{\partial\bar{v}}{\partial\bar{y}}\right) = -\frac{\partial\bar{P}}{\partial\bar{y}} + \frac{1}{\mathrm{Re}}\left(\frac{\partial}{\partial\bar{x}}\left(\frac{\partial\bar{v}}{\partial\bar{x}}\right) + \frac{\partial}{\partial\bar{y}}\left(\frac{\partial\bar{v}}{\partial\bar{y}}\right)\right) \tag{13}$$

$$\left(\bar{u}\frac{\partial\bar{T}}{\partial\bar{x}} + \bar{v}\frac{\partial\bar{T}}{\partial\bar{y}}\right) = \frac{1}{\mathrm{Re}\,\mathrm{Pr}}\left(\frac{\partial}{\partial\bar{x}}\left(\frac{\partial\bar{T}}{\partial\bar{x}}\right) + \frac{\partial}{\partial\bar{y}}\left(\frac{\partial\bar{T}}{\partial\bar{y}}\right)\right) \tag{14}$$

In the above equations, Pr represents the fluid Prandtl number and Re is the flow Reynolds number based on the characteristic length as below:

$$\mathrm{Re} = \frac{\rho U L_c}{\mu} \tag{15}$$

L_o is the channel characteristic length and is equal to 2H.

For solving the momentum and energy equations in the same time, the lattice Boltzmann method is used.

Lattice Boltzmann Method

The distribution function of a particle is in written as [30]:

$$\frac{\partial f}{\partial t} + (c.\nabla) f = \Omega(f) \tag{16}$$

Also the equation of internal energy density distribution function in lattice Boltzmann method is defined as below:

$$\frac{\partial g}{\partial t} + (c.\nabla) g = \Omega(g) \tag{17}$$

Which Ω is the collision term of Boltzmann equation which is defined in the BGK model as below:

$$\Omega(f) = -\frac{f - f^e}{\tau_f} \tag{18}$$

$$\Omega(f) = -\frac{g - g^e}{\tau_g} - fZ \tag{19}$$

where τ_f and τ_g are relaxation times. Also for dealing with problem of discretization, two new distribution functions of $\tilde{f}_i$ and $\tilde{g}_i$ are defined as [31]:

$$\tilde{f}_i = f_i + \frac{dt}{2\tau_f}\left(f_i - f_i^e\right) \tag{20}$$

$$\tilde{g}_i = g_i + \frac{dt}{2\tau_g}\left(g_i - g_i^e\right) + \frac{dt}{2} f_i Z_i \tag{21}$$

Which in here f_i^e and g_i^e are the discrete functions of distribution of the lattice Boltzmann stability for density and internal energy respectively. The subscript symbol of *i* is related to the D2Q9 figure which is shown in figure (1) which is applied in the current work and Z_i is defined as follows [31]:

$$Z_i = (c_i - u).\frac{Du}{Dt} \tag{22}$$

Which in this relation $\frac{Du}{Dt}$ is the total derivative. Furthermore:

$$\begin{aligned} c_i &= \left(\cos\frac{i-1}{2}\pi, \sin\frac{i-1}{2}\pi\right)c, \quad i = 1,2,3,4 \\ c_i &= \sqrt{2}\left(\cos\left[\frac{i-5}{2}\pi + \frac{\pi}{4}\right], \sin\left[\frac{i-5}{2}\pi + \frac{\pi}{4}\right]\right)c, \quad i = 5,6,7,8 \\ c_0 &= (0,0) \end{aligned} \tag{23}$$

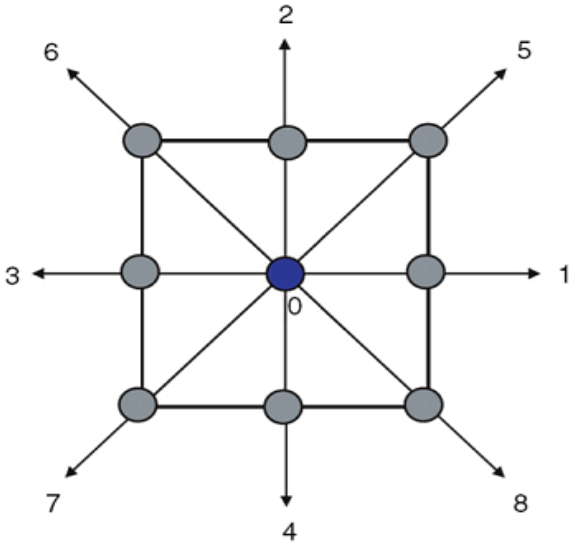

Figure 1. The lattice D2Q9 model [31].

Where c_i is the discretized particle lattice velocity. Also by applying the equilibrium distribution functions of g^e and f^e, the collision and streaming will be in this way [31]:

$$\tilde{f}_i(x + c_i dt, t + dt) - \tilde{f}_i(x,t) = -\frac{dt}{\tau_f + 0.5dt}\left[\tilde{f}_i - f_i^e\right] \tag{24}$$

$$\begin{aligned} \tilde{g}_i(x + c_i dt, t + dt) - \tilde{g}_i(x,t) = &-\frac{dt}{\tau_g + 0.5dt}\left[\tilde{g}_i - g_i^e\right] \\ &-\frac{\tau_g dt}{\tau_g + 0.5dt} f_i Z_i \end{aligned} \tag{25}$$

$$f_i^e = \omega_i \rho\left[1 + \frac{3c_i u}{c^2} + \frac{(3c_i u)^2}{2c^4} - \frac{3\left(u^2 + v^2\right)}{2c^2}\right] \tag{26}$$

$$\begin{aligned} g_0^e &= -\omega_0\left[\frac{3\rho e\left(u^2 + v^2\right)}{2c^2}\right] \\ g_{1,2,3,4}^e &= \omega_1 \rho e\left[1.5 + 1.5\frac{c_i u}{c^2} + 4.5\frac{(c_i u)^2}{c^4} - 1.5\frac{\left(u^2 + v^2\right)}{c^2}\right] \\ g_{5,6,7,8}^e &= \omega_2 \rho e\left[3 + 6\frac{c_i u}{c^2} + 4.5\frac{(c_i u)^2}{c^4} - 1.5\frac{\left(u^2 + v^2\right)}{c^2}\right] \end{aligned} \tag{27}$$

Which in this two dimensional condition for lattice method C^2=3RT=1, ρ_e=ρRT and the weight function is ω_0=1/9 and ω_1=4/9 and ω_2=1/36. Finally, the flow hydraulic and thermal variables are computed in this way [32]:

$$\rho = \sum_i \tilde{f}_i$$
$$\rho u = \sum_i c_i \tilde{f}_i \tag{28}$$
$$\rho e = \sum_i \tilde{g}_i - \frac{dt}{2}\sum_i f_i Z_i$$

Also τ_f and τ_g (relaxation times) are determined as follows:

$$\tau_f = \sqrt{\frac{6}{\pi k}} D_H Kn$$
$$\tau_g = \frac{\tau_f}{\Pr} \tag{29}$$

Boundary Conditions

The boundary conditions have the most defining effect on each problem. As shown in Fig. 2 air at a uniform velocity and temperature is introduced at the inlet. The pressure outlet with zero gauge pressure was set at the outlet of domain. All walls assumed slip condition and temperature jump.

The normal boundary conditions for the input and output of the microchannel is as follows [33]:

$$\tilde{f}_1 = \tilde{f}_3 + \frac{2}{3}\rho_{in}u_{in}$$
$$\tilde{f}_5 = \tilde{f}_7 + \frac{1}{2}\left(\tilde{f}_4 - \tilde{f}_2\right) + \frac{1}{6}\rho_{in}u_{in} \tag{30}$$
$$\tilde{f}_8 = \tilde{f}_6 - \frac{1}{2}\left(\tilde{f}_4 - \tilde{f}_2\right) + \frac{1}{6}\rho_{in}u_{in}$$

$$\tilde{f}_3 = \tilde{f}_1 - \frac{2}{3}\rho_{out}u_{out}$$
$$\tilde{f}_7 = \tilde{f}_5 - \frac{1}{2}\left(\tilde{f}_4 - \tilde{f}_2\right) - \frac{1}{6}\rho_{out}u_{out} - \frac{1}{2}\rho_{out}v_{out} \tag{31}$$
$$\tilde{f}_6 = \tilde{f}_8 + \frac{1}{2}\left(\tilde{f}_4 - \tilde{f}_2\right) - \frac{1}{6}\rho_{out}u_{out} + \frac{1}{2}\rho_{out}v_{out}$$

Also the similar method is used to solve temperature distribution in the microchannel inlet. The function of undefined distribution is computed according to Eq. (32) and in outlet boundary; the boundary condition is defined according to Eq. (33):

$$\tilde{g}_5 = \frac{1}{36}\frac{6\rho e + 3dt\sum_i f_i Z_i - 6\left(\tilde{g}_0 + \tilde{g}_2 + \tilde{g}_3 + \tilde{g}_4 + \tilde{g}_6 + \tilde{g}_7\right)}{2 + 3u_{in} + 3u_{in}^2} \times \left[3 + 6u_{in} + 3u_{in}^2\right]$$
$$\tilde{g}_1 = \frac{1}{9}\frac{6\rho e + 3dt\sum_i f_i Z_i - 6\left(\tilde{g}_0 + \tilde{g}_2 + \tilde{g}_3 + \tilde{g}_4 + \tilde{g}_6 + \tilde{g}_7\right)}{2 + 3u_{in} + 3u_{in}^2} \times \left[1.5 + 1.5u_{in} + 3u_{in}^2\right] \tag{32}$$
$$\tilde{g}_8 = \frac{1}{36}\frac{6\rho e + 3dt\sum_i f_i Z_i - 6\left(\tilde{g}_0 + \tilde{g}_2 + \tilde{g}_3 + \tilde{g}_4 + \tilde{g}_6 + \tilde{g}_7\right)}{2 + 3u_{in} + 3u_{in}^2} \times \left[3 + 6u_{in} + 3u_{in}^2\right]$$

$$\tilde{g}_6 = \frac{1}{36}\frac{6\left(\tilde{g}_1 + \tilde{g}_5 + \tilde{g}_8\right) - 3dt\sum_i\left(\frac{c_{ix}}{c}\right) f_i Z_i - 6\rho e u_{out}}{2 - 3u_{out} + 3u_{out}^2} \times \left[3 - 6u_{out} + 6v_{out} + 3u_{out}^2 + 3v_{out}^2 - 9u_{out}v_{out}\right]$$
$$\tilde{g}_3 = \frac{1}{9}\frac{6\left(\tilde{g}_1 + \tilde{g}_5 + \tilde{g}_8\right) - 3dt\sum_i\left(\frac{c_{ix}}{c}\right) f_i Z_i - 6\rho e u_{out}}{2 - 3u_{out} + 3u_{out}^2} \times \left[1.5 - 1.5u_{out} + 3u_{out}^2 - 1.5v_{out}^2\right] \tag{33}$$

Also on the walls, the velocity slip and temperature jump boundary conditions are considered [33]. The velocity slip boundary conditions on the walls are written as below:

$$\tilde{f}_2 = \tilde{f}_4$$
$$\tilde{f}_{5,6} = r\tilde{f}_{7,8} + (1-r)\tilde{f}_{8,7} \tag{34}$$

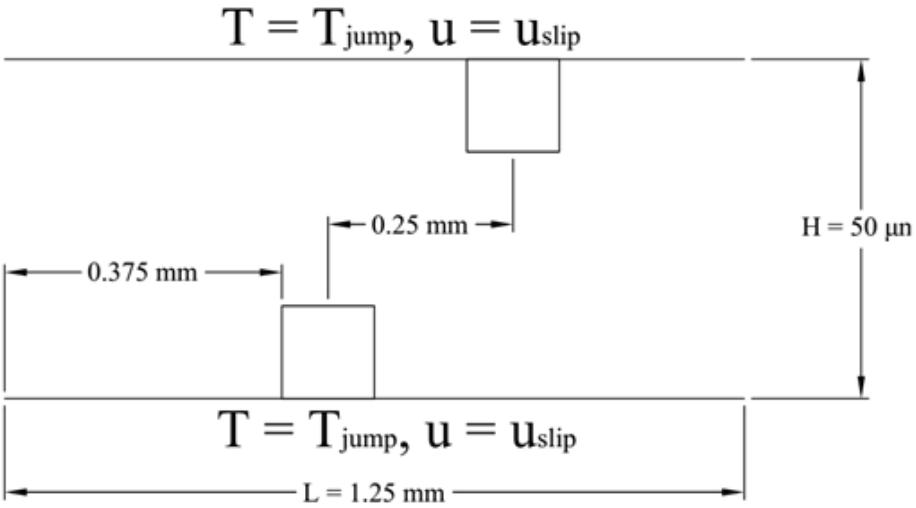

Figure 2. the schematic diagram of geometry.

Where to increase the precision of results, r is chosen less that unity [33]. Also the temperature jump boundary condition will be in this way:

$$\widetilde{g}_{2,5,6} = \frac{3}{\rho_w e} g^e_{2,5,6}\left(\rho_w, u_w, e_w\right)\left(\widetilde{g}_4 + \widetilde{g}_7 + \widetilde{g}_8\right) \quad (35)$$

Which in here ρ_w and u_w are density and velocity on walls respectively.

Problem Geometry

In the current study, the forced convection of nanofluid in a two dimensional rectangle shaped microchannel with presence of two obstacles is investigated. The flow passes through two parallel surfaces and through the space between square obstacles (Figure 2). The channel height is H and the channel length is L, the obstacle dimensions is also $h \times h$, that addition $h=1/4H$. Also the fully developed flow is entered to the microchannel. By considering the fact that the microchannel length ratio is greater to its height, the flow exit as fully developed form from the microchannel. The distance between square shaped obstacles is equal to D. Also the size of the geometry dimensions are shown in figure (2).

Numerical Solution

Lattice Boltzmann method is applied to study the flow and heat transfer of the nanofluid in microchannel. Also the convergence criterion of 10^{-6} is considered. In order to achieve the results independent from the grid, the velocity profile in distance of x=0.4L and in the space between two obstacles is studied according to figure (3). As can be seen in figure (3), the velocity profile in grids with the cellular number of 1500×60 and 2000×80 is almost the same. Hence in order to decrease computational cost in numerical analysis, the grid with cellular number of 1500×60 are applied. In order to ensure that numerical results are independent from computational grid, the mesh independency is examined by using successively smaller cell sizes with a constant factor and mesh generation quality. The grid independence test is conducted for velocity profile for 4 different grid densities as illustrated in Fig. 3. It can be seen that the grid number of 1500×60 is sufficient to ensure the accuracy of the numerical results.

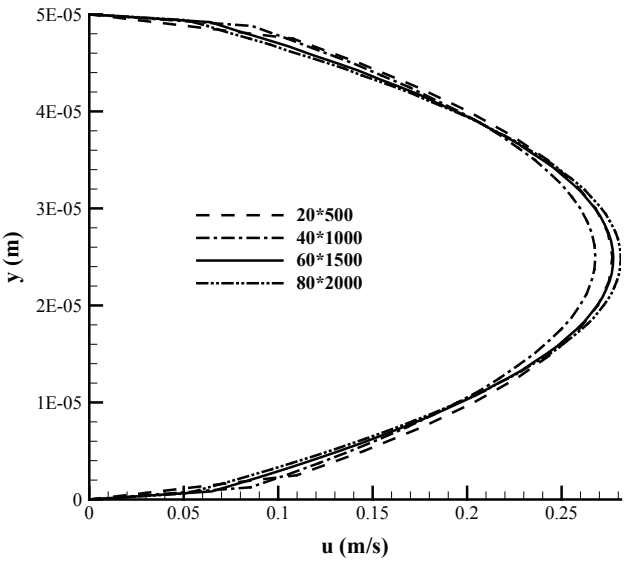

Figure 3. Studying the independence from grid.

In order to study the effect of nanofluid, slip condition and Reynolds number on the heat transfer, the heat transfer coefficient h_x on the lower wall is defined as below:

$$h_x = \frac{q''}{\Delta T} = \frac{\frac{k_{eff}}{k_f} \times \frac{\partial T}{\partial n}}{T_{wall} - T_{bulk}} \quad (36)$$

Too the Nusselt number is determined as follows:

$$Nu = \frac{h_x D_H}{k_{eff}} \quad (37)$$

Also considering the different percentages of nanofluid, studying the friction coefficient of C_f is of high importance. According to that the friction coefficient is computed as below:

$$C_f = \frac{\tau}{\frac{1}{2}\rho u_{in}^2} = \frac{\mu \frac{\partial u}{\partial n}}{\frac{1}{2}\rho u_{in}^2} \quad (38)$$

Validation

Considering the innovation in simulation of nanofluid flow in microchannel and lack of numerical and experimental results as an acceptable standard, in order to study the precision of the results and their validation, the results relating to simulation of the flow through a microchannel and the results relating to simulation of the flow through a channel are validated separately. To verify the accuracy of the numerical model, the simulation results for the flow in a microchannel and in slip condition in two Knudsen numbers of Kn=0.05 and Kn=0.1 with numerical results of Zhang et al. [34] (with permission from Elsevier) are shown in figure (4). Also in order to validate the results about the simulation of a nanofluid in a channel, the results in figure (5) have been compared with results of Santra et al. [22]. (With permission from Elsevier).

RESULTS AND DISCUSSION

In the simulation, the issue of heat transfer and a nanofluid flow passing through a microchannel with presence of two obstacles in the microchannel is studied. The flow and heat transfer for a limited numbers of Reynolds Re and

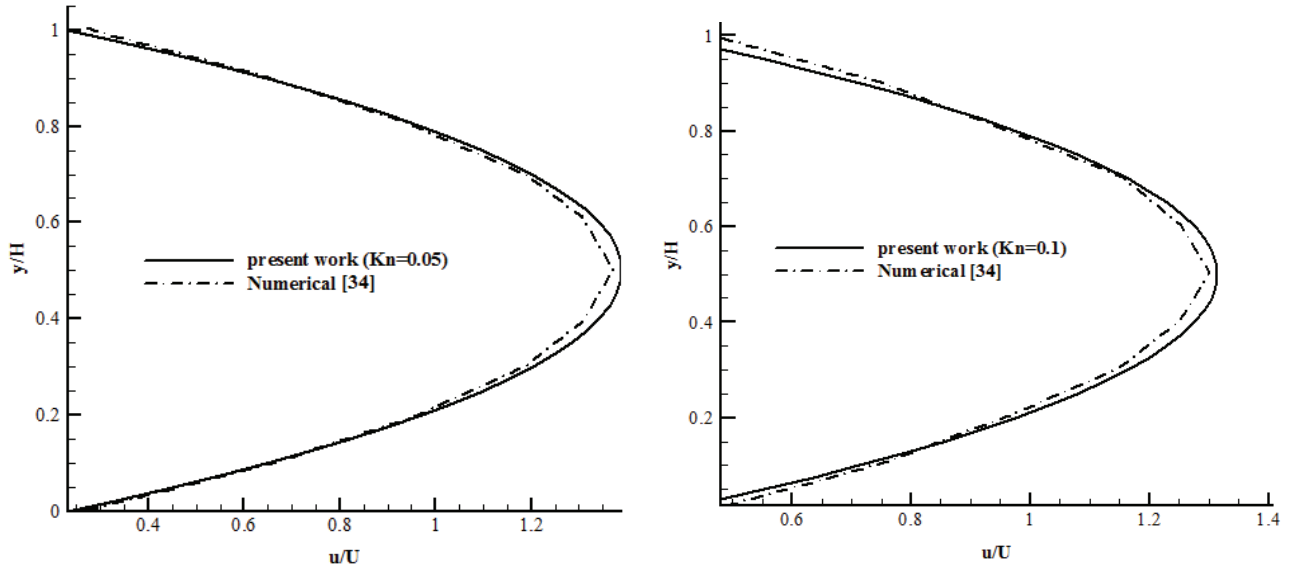

Figure 4. Validation of the developed and dimensionless velocity profile in Kn=0,05, 0,1 with the results of Zhang [34] (With permission from Elsevier).

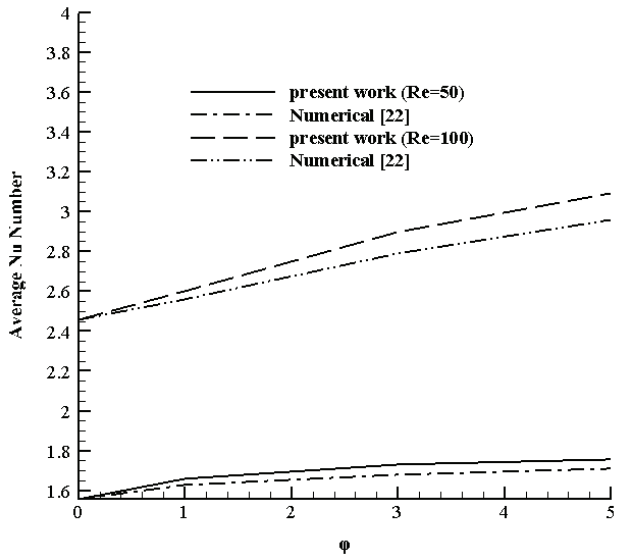

Figure 5. Validation of the Nusselt number according to ϕ=0,3, and 5 in two Reynolds number of 50 and 100 with the results of Santra et al. [22]. (With permission from Elsevier).

Knudsen number Kn and the volume percentage of the nanoparticles (**2**) is studied. The nanofluid is a homogenous mixture of liquid (water) and solid particles (Al_2O_3) which are spherical and the diagonal of each particle is 100 nano meters (100 nm). The simulation are done in three percent of nanoparticle volumes of **2**=0, 3 and 5 and Knudsen numbers of Kn=0.05 and 0.1 and the Reynolds numbers of Re=10, 50. Also considering the effect of heat direction of the nanofluid the study of heat transfer is of a very high importance. That's the reason why the heat transfer coefficient of *h* is used to study the effects of the variance parameters on increase of heat transfer. Also considering the fact the applying any active and inactive method in order to increase the heat transfer coefficient leads to pressure drop and increase of friction coefficient, studying the friction coefficient is also of special importance. In this study considering the fact of adding the nanofluids and increasing the shear tension and friction, the friction coefficient is also studied as well as the heat transfer coefficient. Considering the fact that the heat transfer coefficient and friction coefficient on the square shaped obstacles are also of high importance, the P parameter is defined which is the environment of the higher wall. Hence the results of the coefficient of the heat transfer displacement and friction coefficient are drawn in line with the walls environments which the square obstacles are also considered. Figure (6) shows streamlines in the microchannel. It can be seen that due to existence of square shape obstacles, the permanent vortexes are made which affect the hydraulic and thermal boundary layers and affect the heat transfer and nanofluid flow in the microchannel.

The Effect of Nanoparticles Volume Fraction (ϕ) on Heat Transfer Coefficient

Figure (7) illustrates variations of the heat transfer coefficient with different nanoparticles volume fractions on the lower obstacle's walls of microchannel for different Knudsen numbers in Reynolds number of 10. Also these variations in Reynolds number of 50 is shown in figure (8). According to these figures, the local heat transfer coefficient increases by vortex creation in behind of obstacles

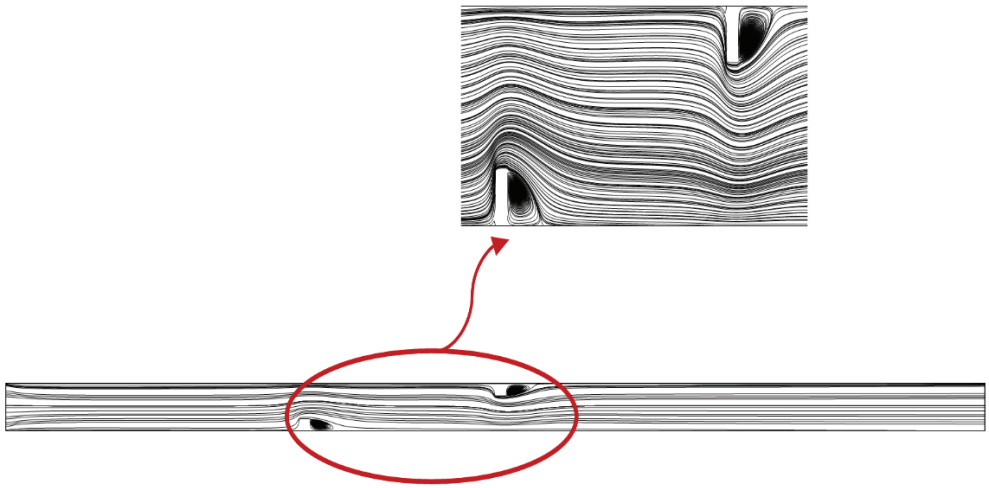

Figure 6. The flow line through a microchannel with magnified display of flow lines around the square obstacles in Re=50, Kn=0.05, ϕ= 5.

which this enhancement is similar for all three nanoparticle volume fractions. This growth is because of the vortexes characteristics and disassembling of the thermal boundary layer in this district. In these districts, the heat transfer coefficient increasing by increasing the nanoparticles volume fraction is less than it by increasing the vortexes. In addition to this, after the first obstacle and in the space between two obstacles and also in the district after the second obstacle, due to existence of rotatory flow which is because of vortex generation by square obstacles, the increase in local heat transfer coefficient is noticeable. It can be seen in figures (7) and (8) that by increasing the nanoparticles volume fraction to 0.03, the heat transfer coefficient becomes 1.5 times greater. Also by increasing it to 0.05, the heat transfer coefficient becomes two times greater than the state without nanoparticles. In addition to this, by increasing the Knudsen number from 0.05 to 0.1, the heat transfer coefficient decreases. This decrease in heat transfer is because of increasing the effect of temperature jump with increasing the Knudsen number. By increasing the Knudsen number and the slippery of the flow and the creation of temperature jump phenomena and the more variance in wall and the fluid near the wall temperature, the heat transfer coefficient will reduces. By comparing figures (7) and (8) and the fact that the studied parameter is studied in a fixed Reynolds number.

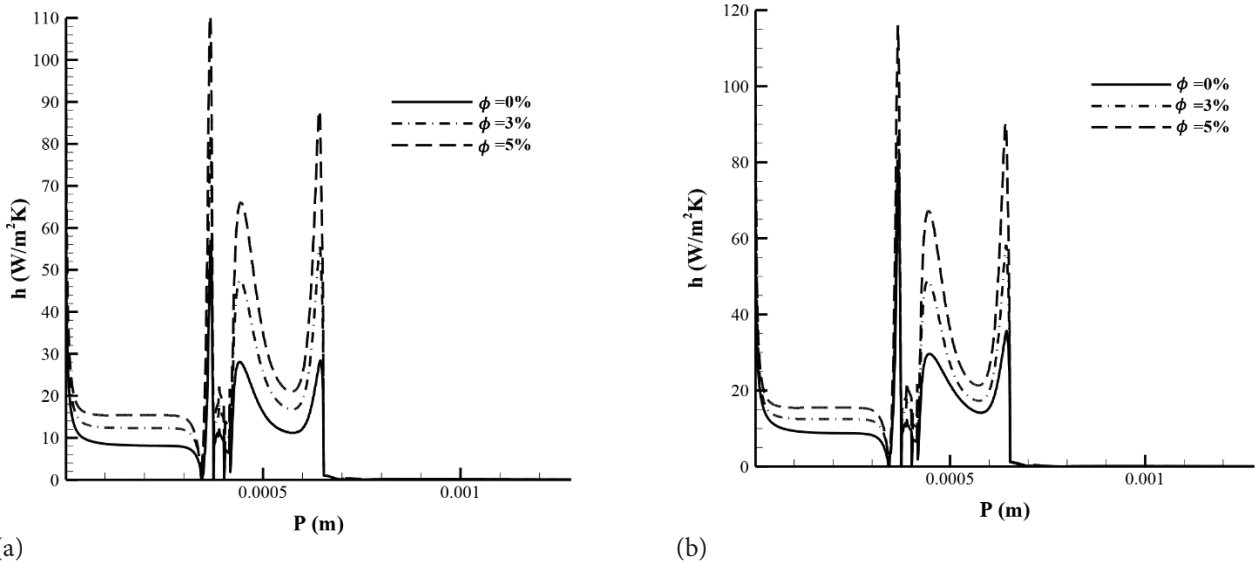

Figure 7. The variation of heat transfer coefficient on the lower wall and obstacle of the microchannel in Re=10, a) Kn=0.05 and b) Kn=0.1.

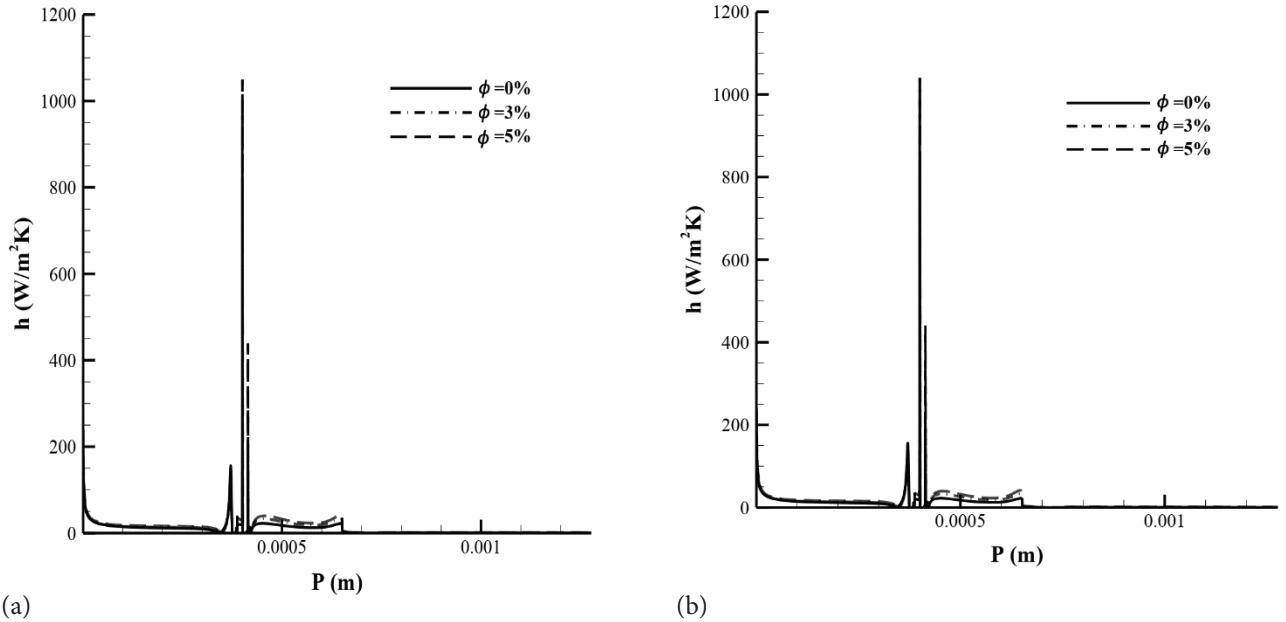

(a) (b)

Figure 8. The variation of heat transfer coefficient on the lower wall and obstacle of the microchannel in Re=50, a) Kn=0.05 and b) Kn=0.1.

It is seen that the Reynolds number of 50 has less heat transfer coefficient than the Reynolds number of 10. In the other hand it is noticed that by increasing the Reynolds number, the effectiveness of the increase in nanoparticles volume fraction decreases. Also this variance between the heat transfer coefficients for two different Reynolds numbers is related to the flow nature and increase in momentum and the hydraulic and thermal boundary layer effects. Mean temperature increases with decreasing Reynolds number, but in other regions, the variation of mean temperature is irregular. It can be found that there is two maximum points for mean temperature just after first heat source for all Reynolds numbers and second heat source.

The Effect of Nanoparticles Volume Fraction (ϕ) on Friction Coefficient on the Wall

Figures (9) and (10) illustrate the variations of friction coefficient with different nanoparticle volume fractions on the lower obstacle's walls of microchannel for different Knudsen numbers in Reynolds numbers of 10 and 50, respectively. According to these figures it is observed that

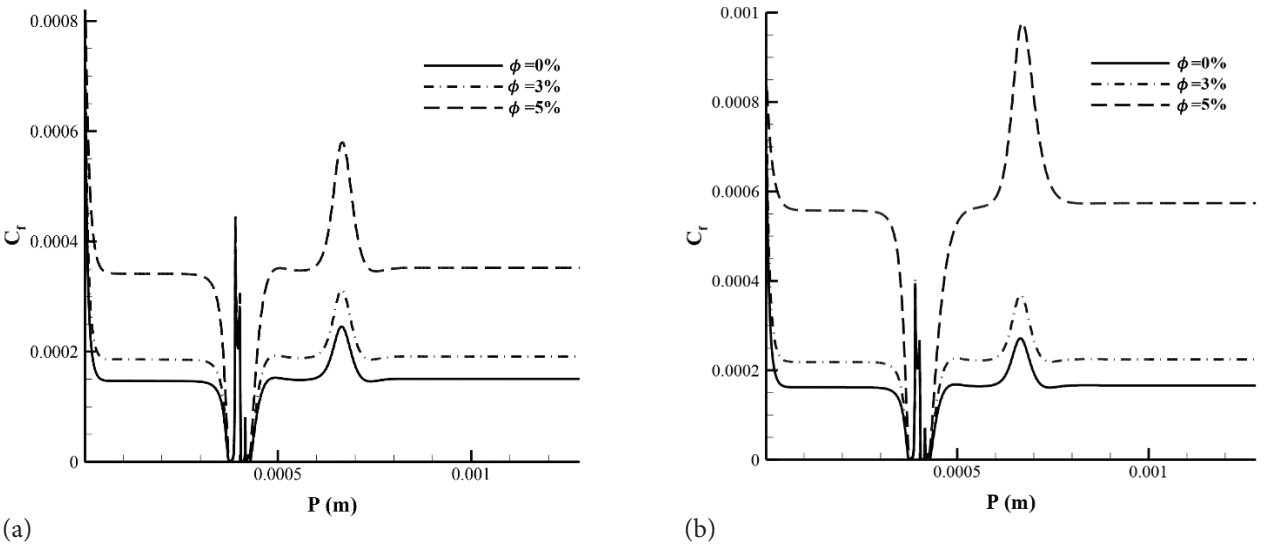

(a) (b)

Figure 9. Variation of the friction coefficient on the lower wall and obstacle of the microchannel in Re=10 in a) Kn=0.05, Kn=0.1.

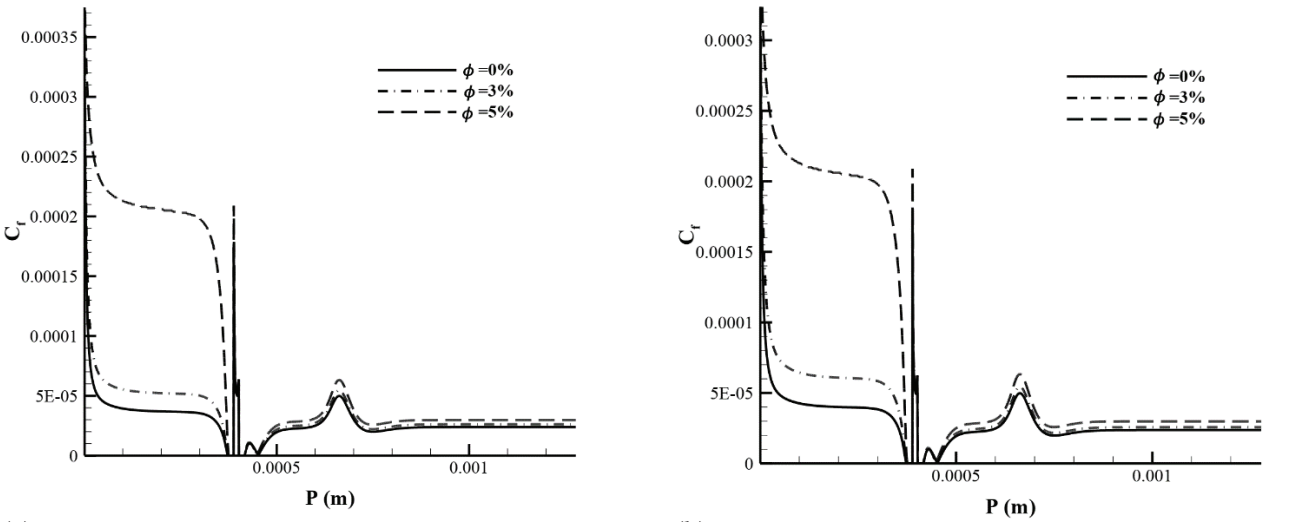

Figure 10. Variation of the friction coefficient on the lower wall and obstacle of the microchannel in Re=50 in a) Kn=0.05 and b) Kn=0.1.

by increasing the nanoparticles volume fraction (ϕ), the friction coefficient rises. This rise is because of the shear stress enhancement due to increase of effective viscosity of the nanofluid and the Brownian energy and increase of friction in the fluid flow. Also as it is clear from these figures, the friction coefficient has a maximum and noticeable enhancement near the obstacles. This positional increase is because of the sudden rise of the shear stress around the square obstacles. Due to existence of vortexes in the back of the square obstacles and generating rotatory flow and vortexes in this district, the shear stress raises intensively that leads to the friction coefficient rise. Also after the second obstacle and after the development of the velocity and according to the stability of the velocity profile through x, the shear stress and the friction coefficient became fixed. In addition it is observed that by increasing the Knudsen number, the friction coefficient in a fixed Reynolds number and a fixed nanoparticles volume fraction have reduced. This decrease takes place because of the fact that the flow has more slips with increasing the Knudsen number, which leads to less shear stress. With increasing Kn-number, difference Nusselt number is increased between first and second heat sources. As it can be seen the average Nusselt number is increased with increasing Knudsen number for first heat source but it's decreased with increasing Knudsen number for second heat source, in other words, convection heat transfer is decreased while conduction heat transfer is becomes more significant. Also by comparing figures 9 and 10 and studying the Reynolds number parameter in a stable ϕ and Kn, it is concluded that by raising the Reynolds number the friction coefficient decreases. This decrease is because of the flow momentum rise which makes the hydraulic boundary layer thinner.

CONCLUSION

In this study, the slip flow of a nanofluid is studied in a microchannel with the presence of two obstacles using lattice Boltzmann method. The velocity slip and temperature jump boundary conditions are used for the simulations. The nanofluid is made up of water and percentages of different volume fractions of aluminum dioxide (Al_2O_3) nanoparticles. In order to make difference in nanofluid characteristics, a stable temperature distribution on the upper and lower walls is applied.

The simulations are conducted for three volume fraction of nanoparticles is 0 and 0.03, and 0.05, the Knudsen number is 0, 0.05, and 0.1, and Reynolds number is 10 and 50. The following results can be summarized:

- It is observed that by increasing the Knudsen number, the velocity slip and also temperature jump increases, but the heat transfer coefficient and the friction coefficient decreases.
- The first obstacle in the microchannel is more effective which is due to the creation of the vortex and the vortex characteristics in dissembling the hydraulic and thermal boundary layers.
- It is observed that by increasing the nanoparticles volume fraction, the heat transfer coefficient rises noticeably. In the other hand the friction coefficient also rises by increasing the nanoparticles volume fraction.
- By increasing the Reynolds number, the heat transfer coefficient increases and the friction coefficient decreases. In the other hand, it is observed that by increasing the Reynolds number, the effectiveness of nanoparticles volume fraction rise decreases.
- With increasing Kn-number, difference Nusselt number is increased between first and second heat sources.

- Mean temperature increases with decreasing Reynolds number, but in other regions, the variation of mean temperature is irregular. It can be found that there is two maximum points for mean temperature just after first heat source for all Reynolds numbers and second heat source.

NOMENCLATURE

A	Ratio of applied external voltage to the base voltage
B	Ratio of ion pressure to dynamic pressure
e	Electron charge [C]
E	Strength of external field [V/m]
H	Height of microchannel [m]
k	Thermal conductivity coefficient
K_B	Boltzmann constant [j/K]
κ	Debye-Huckel parameter [$1/m$]
L	Length of microchannel [m]
nf	Nanofluid
n_0	ion concentration [$ions/m^3$]
P	Pressure [pa]
Pr	Prandtl number
Re	Reynolds number
Z	Valance number
T	Temperature [K]
ρ	density[Kg/m^3]
ν	Kinetic viscous[m^3/s]
τ	Relaxation time
μ	Dynamic viscous[Kg/s]
d	Diameter[m]
s	Solid
f	fluid
V	Velocity vector[m/s]
c_p	Specific heat capacity [$J/Kg.K$]
f	Density distribution function
g	Temperature distribution function
h	Electric potential distribution function
α	Thermal penetration coefficient [m^2/s]
D	Hydraulic diameter
f^{eq}	Maxwell-Boltzmann equilibrium distribution function
C_s	Sound velocity in the medium
c	Velocity of data transfer in the network
Nu	Nusselt number
ζ	Electric potential of wall [V]
ψ	Distribution of electric potential
ϕ	Electric potential
Ω	Collision term of Boltzmann equation
ε_r	Electric permeability ratio versus vacuum
ε_0	Electric permeability in vacuum [C/Vm]
ε	Internal energy per mass unit
U_{HZ}	Helmhotz – Smocholofski velocity[m/s]
φ	Volume fraction
w_i	Weight function
e_i	Microscopic velocity vector
Kn	Knudsen number

AUTHORSHIP CONTRIBUTIONS

Authors equally contributed to this work.

DATA AVAILABILITY STATEMENT

The authors confirm that the data that supports the findings of this study are available within the article. Raw data that support the finding of this study are available from the corresponding author, upon reasonable request.

CONFLICT OF INTEREST

The author declared no potential conflicts of interest with respect to the research, authorship, and/or publication of this article.

ETHICS

There are no ethical issues with the publication of this manuscript.

STATEMENT ON THE USE OF ARTIFICIAL INTELLIGENCE

Artificial intelligence was not used in the preparation of the article.

REFERENCES

[1] İlikan AN, Aydın R. Analysis of the slip flow in the hydrodynamic entrance region of a 2D microchannel. J Therm Eng 2023;9:733–45. [CrossRef]

[2] Anwar T, Kumam P, Thounthong P, Sitthithakerngkiet K. Nanoparticles shape effects on thermal performance of Brinkman-type ferrofluid under heat injection/consumption and thermal radiation: A fractional model with non-singular kernel and non-uniform temperature and velocity conditions. J Mol Liq 2021;335:116107. [CrossRef]

[3] Anwar T, Kumam P, Muhammad S. New fractional model to analyze impacts of Newtonian heating, shape factor and ramped flow function on MgO–SiO_2–kerosene oil hybrid nanofluid. Case Stud Therm Eng 2022;38:102361. [CrossRef]

[4] Asadollahi A, Rashidi S, Esfahani JA. Simulation of liquid reaction and droplet formation on a moving micro-object by lattice Boltzmann method. Meccanica 2018;53:803–15. [CrossRef]

[5] Muhammad S, Anwar T, Asifa, Yavuz M. Comprehensive investigation of thermal and flow features of alloy-based nanofluid considering shape and Newtonian heating effects via new fractional approach. Fractals Fract 2023;7:150. [CrossRef]

[6] Asifa, Anwar T, Kumam P, Shah Z, Sitthithakerngkiet K. Significance of shape factor in heat transfer performance of molybdenum-disulfide nanofluid in multiple flow situations; A comparative fractional study. Molecules 2021;26:3711. [CrossRef]

[7] Anwar T, Asifa, Kumam P, El-Zahar ER, Muhammad S, Seddek LF. Thermal analysis of mineral oil-based hybrid nanofluid subject to time-dependent energy and flow conditions and multishaped nanoparticles. J Therm Anal Calorim 2024;149:6813−36. [CrossRef]
[8] Ezzatneshan E, Salehi A, Vaseghnia H. Study on forcing schemes in the thermal lattice Boltzmann method for simulation of natural convection flow problems. Heat Transf 2021;50:7604−31. [CrossRef]
[9] Chamkha AJ, Abbasbandy S, Rashad AM, Vajravelu K. Radiation effects on mixed convection about a cone embedded in a porous medium filled with a nanofluid. Meccanica 2013;48:275−85. [CrossRef]
[10] Arabpour A, Karimipour A, Toghraie D, Akbari OA. Investigation into the effects of slip boundary condition on nanofluid flow in a double-layer microchannel. J Therm Anal Calorim 2018;131:2975−91. [CrossRef]
[11] Abbassi MA, Djebali R, Guedri K. Effects of heater dimensions on nanofluid natural convection in a heated incinerator shaped cavity containing a heated block. J Therm Eng 2018;4:2018−36. [CrossRef]
[12] Lv Y, Liu S. Topology optimization and heat dissipation performance analysis of a micro-channel heat sink. Meccanica 2018;53:3693−708. [CrossRef]
[13] Zade AQ, Renksizbulut M, Friedman J. Heat transfer characteristics of developing gaseous slip-flow in rectangular microchannels with variable physical properties. Int J Heat Fluid Flow 2011;32:117−27. [CrossRef]
[14] Eckstein Y, Yossifon G, Seifert A, Miloh T. Nonlinear electrokinetic phenomena around nearly insulated sharp tips in microflows. J Colloid Interface Sci 2009;338:243−9. [CrossRef]
[15] Sharp KV, Yazdi SH, Davison SM. Localized flow control in microchannels using induced-charge electroosmosis near conductive obstacles. Microfluid Nanofluidics 2011;10:1257−67. [CrossRef]
[16] Bera S, Bhattacharyya S. Electroosmotic flow in the vicinity of a conducting obstacle mounted on the surface of a wide microchannel. Int J Eng Sci 2015;94:128−38. [CrossRef]
[17] Roy G, Nguyen CT, Lajoie PR. Numerical investigation of laminar flow and heat transfer in a radial flow cooling system with the use of nanofluids. Superlattices Microstruct 2004;35:497−511. [CrossRef]
[18] Ho CJ, Wei LC, Li ZW. An experimental investigation of forced convective cooling performance of a microchannel heat sink with Al_2O_3/water nanofluid. Appl Therm Eng 2010;30:96−103. [CrossRef]
[19] Tsai TH, Chein R. Performance analysis of nanofluid-cooled microchannel heat sinks. Int J Heat Fluid Flow 2007;28:1013−26. [CrossRef]
[20] Jang SP, Choi SU. Cooling performance of a microchannel heat sink with nanofluids. Appl Therm Eng 2006;26:2457−63. [CrossRef]
[21] Alipour Lalami A, Kalteh M. Lattice Boltzmann simulation of nanofluid conjugate heat transfer in a wide microchannel: Effect of temperature jump, axial conduction and viscous dissipation. Meccanica 2019;54:135−53. [CrossRef]
[22] Santra AK, Sen S, Chakraborty N. Study of heat transfer due to laminar flow of copper−water nanofluid through two isothermally heated parallel plates. Int J Therm Sci 2009;48:391−400. [CrossRef]
[23] Rajan I, Perumal DA. Flow dynamics of lid-driven cavities with obstacles of various shapes and configurations using the lattice Boltzmann method. J Therm Eng 2021;7:83−102. [CrossRef]
[24] Bamdad K, Ashorynejad HR. Inverse analysis of a rectangular fin using the lattice Boltzmann method. Energy Convers Manag 2015;97:290−7. [CrossRef]
[25] Agarwal RK, Chusak L. Lattice Boltzmann simulations of slip flow of non-Newtonian fluids in microchannels. In: Hirschel EH, Periaux J, Satofuka N, editors. Parallel computational fluid dynamics 2008: Parallel numerical methods, software development and applications. Berlin: Springer; 2010. p. 247−56. [CrossRef]
[26] Navidbakhsh M, Rezazadeh M. A computational study of a capsule lateral migration in microchannel flow. Acta Mech Sin 2013;29:513−25. [CrossRef]
[27] Javaherdeh K, Karimi H. Numerical analysis of mixed convection of sodium alginate non-Newtonian fluid with Al_2O_3 nanoparticle in a channel with block. J Appl Comput Sci Mech 2021;32:93−110.
[28] Huminic G, Huminic A. Entropy generation of nanofluid and hybrid nanofluid flow in thermal systems: A review. J Mol Liq 2020;302:112533. [CrossRef]
[29] Izadi M, Mohammadi SA, Mehryan SAM, Yang T, Sheremet MA. Thermogravitational convection of magnetic micropolar nanofluid with coupling between energy and angular momentum equations. Int J Heat Mass Transf 2019;145:118748. [CrossRef]
[30] Javaherdeh K, Karimi H, Azarbarzin T. Lattice Boltzmann simulation of fluid flow and heat transfer in a microchannel with heat sources located on the walls. Superlattices Microstruct 2021;160:107069. [CrossRef]
[31] Gokaltun S, Dulikravich GS. Lattice Boltzmann computations of incompressible laminar flow and heat transfer in a constricted channel. Comput Math Appl 2010;59:2431−41. [CrossRef]
[32] Tian ZW, Zou C, Liu HJ, Guo ZL, Liu ZH, Zheng CG. Lattice Boltzmann scheme for simulating thermal micro-flow. Physica A. 2007;385:59−68. [CrossRef]
[33] Chang C, Liu CH, Lin CA. Boundary conditions for lattice Boltzmann simulations with complex geometry flows. Comput Math Appl 2009;58:940−9. [CrossRef]
[34] Zhang YH, Qin RS, Sun YH, Barber RW, Emerson DR. Gas flow in microchannels−a lattice Boltzmann method approach. J Stat Phys 2005;121:257−67. [CrossRef]